doi:10.1093/brain/awv357 BRAIN 2016: 139; 338–345 | 338

BRAIN
A JOURNAL OF NEUROLOGY

REPORT

Loss of the smallest subunit of cytochrome c oxidase, COX8A, causes Leigh-like syndrome and epilepsy

Kerstin Hallmann,[1] Alexei P. Kudin,[1] Gábor Zsurka,[1] Cornelia Kornblum,[2] Jens Reimann,[2] Burkhard Stüve,[3] Stephan Waltz,[3] Elke Hattingen,[4] Holger Thiele,[5] Peter Nürnberg,[5,6,7] Cornelia Rüb,[8] Wolfgang Voos,[8] Jens Kopatz,[9] Harald Neumann[9] and Wolfram S. Kunz[1]

Isolated cytochrome *c* oxidase (complex IV) deficiency is one of the most frequent respiratory chain defects in humans and is usually caused by mutations in proteins required for assembly of the complex. Mutations in nuclear-encoded structural subunits are very rare. In a patient with Leigh-like syndrome presenting with leukodystrophy and severe epilepsy, we identified a homozygous splice site mutation in *COX8A*, which codes for the ubiquitously expressed isoform of subunit VIII, the smallest nuclear-encoded subunit of complex IV. The mutation, affecting the last nucleotide of intron 1, leads to aberrant splicing, a frame-shift in the highly conserved exon 2, and decreased amount of the *COX8A* transcript. The loss of the wild-type COX8A protein severely impairs the stability of the entire cytochrome *c* oxidase enzyme complex and manifests in isolated complex IV deficiency in skeletal muscle and fibroblasts, similar to the frequent c.845_846delCT mutation in the assembly factor *SURF1* gene. Stability and activity of complex IV could be rescued in the patient's fibroblasts by lentiviral expression of wild-type *COX8A*. Our findings demonstrate that COX8A is indispensable for function of human complex IV and its mutation causes human disease.

1 Department of Epileptology and Life and Brain Centre, University of Bonn, Bonn, Germany
2 Department of Neurology, University of Bonn, Bonn, Germany
3 Children's Hospital Cologne, Cologne, Germany
4 Department of Radiology, Division of Neuroradiology, University of Bonn, Bonn, Germany
5 Cologne Centre for Genomics (CCG), University of Cologne, Cologne, Germany
6 Centre for Molecular Medicine Cologne (CMMC), University of Cologne, Cologne, Germany
7 Cologne Excellence Cluster on Cellular Stress Responses in Aging-Associated Diseases (CECAD), University of Cologne, Cologne, Germany
8 Institut für Biochemie und Molekularbiologie, University of Bonn, Bonn, Germany
9 Neural Regeneration Group, Institute of Reconstructive Neurobiology, University of Bonn, Bonn, Germany

Correspondence to: Dr Wolfram S. Kunz,
Division of Neurochemistry,
Department of Epileptology and Life and Brain Centre,
University Bonn Medical Centre,
Sigmund-Freud-Str. 25,
D-53105 Bonn,
Germany
E-mail: wolfram.kunz@ukb.uni-bonn.de

Keywords: Leigh-like syndrome; mitochondrial disease; cytochrome *c* oxidase; subunit COX VIIIa

Abbreviation: COX = cytochrome *c* oxidase

Received July 14, 2015. Revised September 30, 2015. Accepted October 21, 2015. Advance Access publication December 18, 2015

Introduction

Cytochrome *c* oxidase (COX) is the terminal enzyme complex of the respiratory chain and catalyses the transfer of electrons from cytochrome *c* to oxygen coupled to proton pumping from the mitochondrial matrix to the intermembrane space. Isolated COX deficiency (MIM 220110), one of the most frequent respiratory chain defects in humans, is usually caused by mutations in genes coding for proteins required for translation or maturation of mitochondrial-encoded COX subunits or assembly of the complex (Soto *et al.*, 2012). Mutations affecting structural subunits of complex IV have been very rarely described to be associated with disease. To date, mutations in four structural subunits of COX [*COX6A1* (Tamiya *et al.*, 2014), *COX6B1* (Massa *et al.*, 2008; Abdulhag *et al.*, 2015), *COX4I2* (Shteyer *et al.*, 2009), and *COX7B* (Indrieri *et al.*, 2012)] have been reported. Furthermore, mutations in *NDUFA4* (Pitceathly *et al.*, 2013), a gene that encodes a protein that was previously assigned to complex I, but recently claimed to be an additional COX subunit, also leads to a mitochondrial disease. Here, we describe a patient with a multisystemic Leigh-like syndrome associated with severe isolated COX deficiency in skeletal muscle and fibroblasts due to a homozygous splice site mutation in *COX8A*. This mutation leads to a loss of functional COX8A protein. Our data show that this small nuclear-encoded structural subunit is indispensable for stability and activity of the cytochrome *c* oxidase complex.

Materials and methods

Patients

The female *COX8A* patient was the child of parents of Turkish origin. Consanguinity was not known, but was suggested by genetic data. She was born after an uneventful pregnancy and delivery at normal gestational age. A congenital scoliosis with thoracolumbar kyphosis and bilateral *pes planovalgus* were present at birth. Primary developmental delay and primary pulmonary hypertension were diagnosed at the age of 6 months. At the age of 4–5 years, a cachectic appearance with malnutrition and recurrent vomiting was evident, and a percutaneous gastrointestinal feeding tube was inserted. At the age of 8 years, the girl presented with a febrile state due to pneumonia and urinary tract infection, which resulted in the first manifestation of focal and generalized epileptic tonic-clonic seizures and a severe metabolic crisis with lactic acidosis. Further clinical phenotyping and diagnostic procedures showed serious psychomotor retardation, a short stature, microcephalus, enophthalmus, proximal muscular hypotonia, distal spasticity of upper and lower limbs, weak deep tendon reflexes, and absent extensor plantar responses. At the age of 10 years, a dislocation of both hips was diagnosed. Meanwhile, the patient was non-ambulatory and wheelchair-bound. Her severe epilepsy presented with tonic-clonic, myoclonic, and atonic seizures and only partly responded to various antiepileptic drug treatment regimens including levetiracetam, oxcarbazepine, and sultiame. Pneumonia with sepsis manifested at the age of 12 years resulting in a serious metabolic crisis and cardiorespiratory failure. The patient died after several weeks of intensive care unit treatment after unsuccessful cardiopulmonary resuscitation at the age of 12.5 years.

Diagnostic work-up at the age of 8 years showed pathological EEG changes with generalized slowing and continuous multifocal spike-and-wave activity. Elevated lactate levels were present in the CSF (max. 11.4 mmol/l, normal values <2) and peripheral blood (max. 6.2 mmol/l, normal values <1.6). Metabolic screening of the urine and CSF showed elevated lactate and citric acid cycle metabolite levels, as well as increased glycine and alanine levels. Ophthalmological examinations detected a pigmentary retinopathy.

Brain MRI at the age of 8 years (Fig. 1A) showed a left-sided small lacunar thalamic lesion without further basal ganglia or cortical signal alterations, signal hyperintensities in T_2-weighted sequences in the right cerebellar hemisphere. Diffusion-weighted imaging revealed extensive and symmetric areas of restricted diffusion in the white matter that were first interpreted as encephalitis or metabolic encephalopathy. A subsequent brain MRI at the age of 12 years (Fig. 1B) showed a progressive and extent atrophy especially of the white matter with white matter signal changes in T_2-weighted sequences that were most pronounced in periventricular areas, cerebellar hemispheres, and parietooccipital lobes. A consecutive biventricular *ex vacuo* enlargement and cystic defects with parietooccipital predominance were also detected.

SURF1-deficient fibroblasts and the corresponding skeletal muscle biopsy sample were from a 3-year-old girl of Saudi Arabian origin harbouring the homozygous c.845_846delCT mutation in the *SURF1* gene. Control muscle and skin specimens were obtained from 28 patients who underwent a muscle biopsy for diagnosis of neuromuscular symptoms but were ultimately deemed to be normal by means of combined clinical, electrophysiological, and histological criteria. Written informed consent was obtained from the parents of the patients and all investigations were carried out according to the guidelines of the Ethical committee of the University Bonn Medical Centre.

Histological and immunohistological investigations

Histological investigations of open skeletal muscle biopsies (vastus lateralis muscles) of the patients were performed according to protocols described by Dubowitz and Sewry (2007). For immunohistochemical visualization of respiratory chain enzyme complexes, an antibody against the 15 kDa subunit of complex I (NDUFS5; Molecular Probes, A31856, clone 17G3) and an antibody against the subunit 1 of COX (MT-CO1; Molecular Probes, A6403, clone 1D6) were used. To determine the efficiency of viral transduction in fibroblasts, we used an anti-DDK antibody from OriGene Technologies.

Cell culture conditions

Fibroblasts from 5×5 mm skin biopsies of both patients were cultivated in high-glucose (4.5 g/l) Dulbecco's modified Eagle

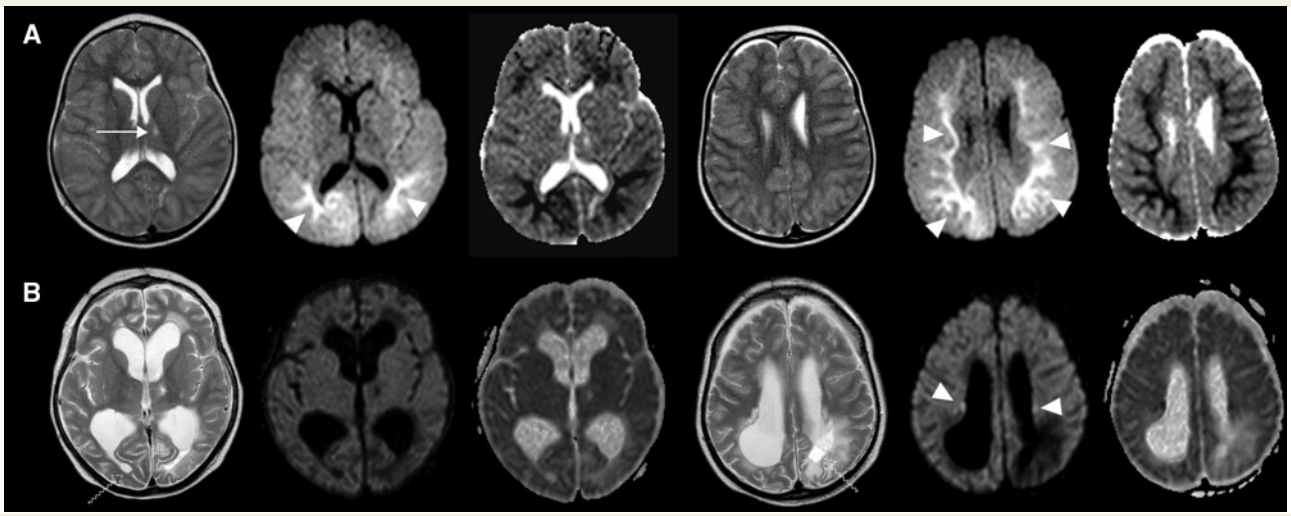

Figure 1 Brain MRI of the index patient at the ages of 8 and 12.5 years. From *left* to *right*: Axial T_2, apparent diffusion coefficient (ADC) and diffusion-weighted imaging (DWI) sequences (at two different layers, respectively). (**A**) Brain MRI at 8 years of age. Small lacunar thalamic lesion (arrow) without ADC reduction and without further basal ganglia or cortical signal alterations, T_2-weighted sequences. Symmetric extent and diffuse signal increases of the white matter with periventricular predominance, DWI sequences. ADC maps show an ADC decrease in the corresponding white matter (arrowheads). (**B**) Brain MRI at 12.5 years of age. Biventricular *ex vacuo* hydrocephalus, brain atrophy with rarefication of the white matter, extent symmetric white matter signal changes most pronounced in periventricular areas and parietooccipital lobes, in part with cystic appearance on T_2-weighted sequences (dashed arrows). Some patchy white matter areas show an increased signal in DWI sequences compatible with an ongoing process of white matter affection (arrowhead).

medium with pyruvate and glutamine (PAA Laboratories) supplemented with 10% foetal calf serum, 100 U/ml penicillin, 100 U/ml streptomycin, and 50 mg/l uridine in a 6.5% CO_2 atmosphere at 37°C. Cells were harvested after passage 11 or 12 and suspended in phosphate-buffered saline.

Enzyme activity, respiration measurements and blue native polyacrylamide gel electrophoresis

The activity of citrate synthase, rotenone-sensitive NADH:CoQ_1 oxidoreductase, and COX was determined by standard methods (Wiedemann *et al.*, 2000). The details on the performed biochemical assays are outlined in the Supplementary material.

DNA and RNA samples, molecular biology techniques and lentiviral rescue of *COX8A*

Genomic DNA was isolated from 10 ml aliquots of EDTA-anticoagulated blood by a salting-out technique (Miller *et al.*, 1988). Total fibroblast RNA was obtained by disrupting cells in TRIzol® Reagent (Life Technologies) followed by isolation of the RNA with the RNeasy® MiniKit (Qiagen). Tissue-specific expression of *COX8A* and *COX8C* was investigated using the Human Multiple Tissue cDNA Panel 1 from Clontech Laboratories, Inc., and FirstChoice® Human Brain Total RNA from testis (Ambion). Complementary DNA was produced from RNA templates with the iScript™ Select cDNA synthesis kit (Bio-Rad) using random primers for reverse transcription. The details on polymerase chain reaction (PCR) amplification, whole exome sequencing and lentiviral rescues of *COX8A* are outlined in the Supplementary material.

Statistical analysis

The results are presented as mean ± standard deviation (SD). Significant changes were assessed by Student's *t*-test, with $P < 0.05$ as the level of significance.

Results

Biochemical analysis of skeletal muscle and fibroblast homogenates of a patient with microcephalus, serious psychomotor retardation and severe epilepsy (Supplementary Tables 1 and 2) showed an isolated deficiency of COX activity in both tissues. A uniformly distributed weak COX staining was visible in the skeletal muscle biopsy (Fig. 2, middle), even more severe as observed for a patient with a homozygous frame shift mutation in *SURF1*, an assembly factor of COX (Fig. 2). The respiration activities, determined in digitonin-permeabilized fibroblasts (Supplementary Table 3), also support the isolated COX deficiency in the *COX8A* patient, rather similar to the data obtained from a patient harbouring the *SURF1* mutation. While the endogenous respiration activities were nearly unaltered, the ADP supported respiration with all tested substrate combinations were approximately two times lower than the corresponding control values. Moreover, the maximal respiratory activity showed

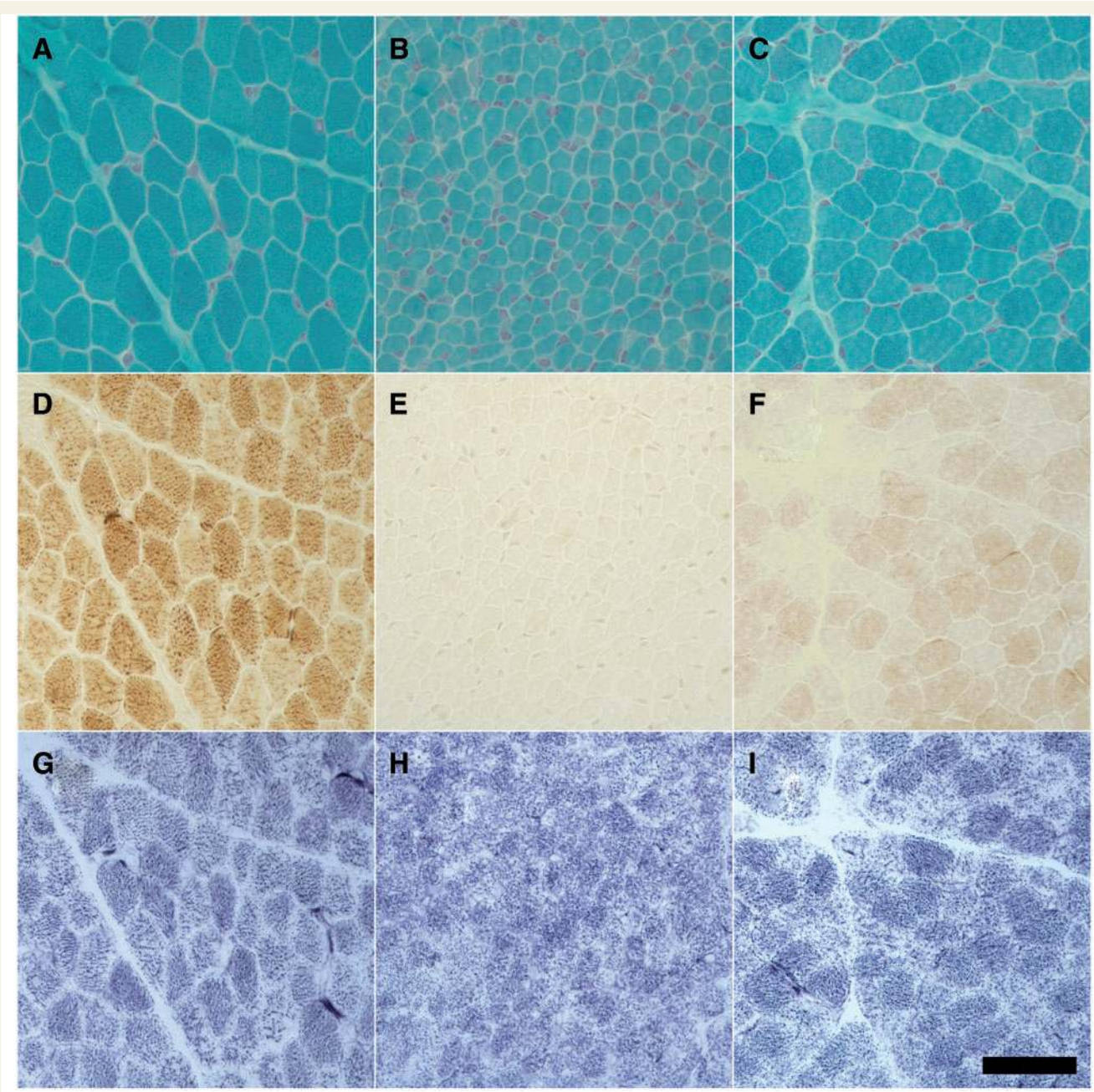

Figure 2 Decreased COX activity in skeletal muscle due to *COX8A* and *SURF1* mutations. Muscle histochemistry from a control subject (**A**, **D** and **G**), the *COX8A* patient (**B**, **E** and **H**) and a patient harbouring the homozygous c.845_846delCT *SURF1* mutation (**C**, **F** and **I**). (**A–C**) Gomori's trichrome; (**D–F**) cytochrome *c* oxidase; (**G–I**) succinate dehydrogenase. Scale bar = 50 μm.

an elevated sensitivity to the COX inhibitor azide, corresponding to an increased flux control coefficient of cytochrome *c* oxidase (Kuznetsov *et al.*, 1997).

Whole exome sequencing of the index patient revealed rare homozygous missense variants in 19 genes (Supplementary Table 4) and one splice site mutation, among which only the c.115-1G>C splice acceptor site mutation in *COX8A* (Fig. 3A) could be attributed to a mitochondrial protein (Mitocarta). Among the detected missense mutations only the *BCAN* p.G720S mutation reached a CADD score >27, but was not considered being relevant for the disease because brevican-deficient mice show no obvious phenotypic abnormality (Brakebusch *et al.*, 2002). To confirm aberrant splicing that was predicted by the position of the *COX8A* mutation, we amplified the cDNA of a large part of the *COX8A* transcript with primers located in the 5' and 3'-end untranslated regions. To detect, in parallel, the transcript of the other human *COX8* gene, *COX8C*, we performed multiplex PCR (Fig. 3B). In line with the reported

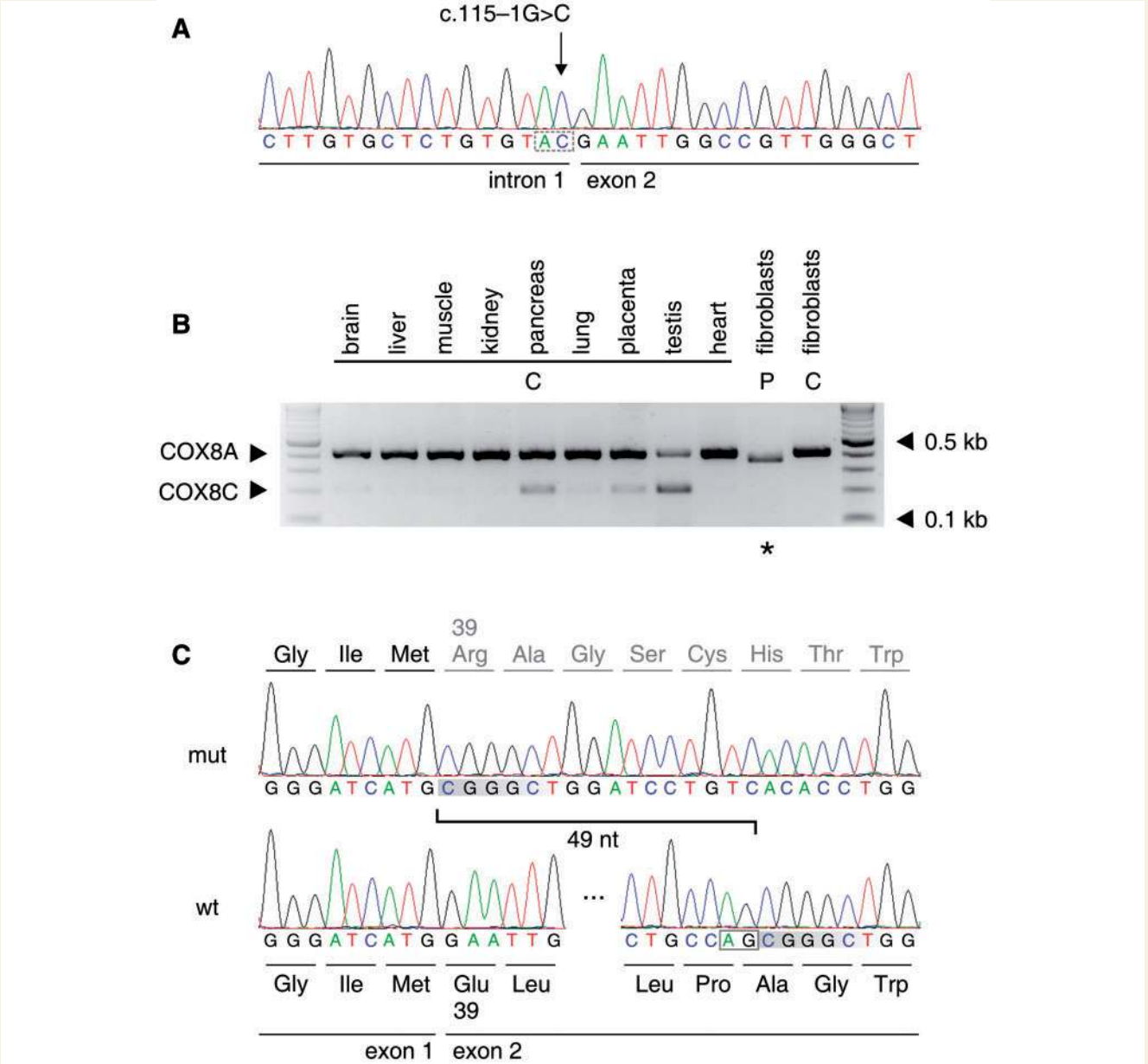

Figure 3 Consequences of the c.115-1G>C splice site mutation on mRNA level. (**A**) Confirmation of the homozygous c.115-1G>C *COX8A* splice acceptor site mutation by conventional Sanger sequencing. The disrupted acceptor motive is indicated by the dashed box. (**B**) Multiplex PCR detection of *COX8A* and *COX8C* expression in different tissues. The upper band represents the *COX8A* transcript, the lower band the *COX8C* transcript. The asterisk indicates the shorter *COX8A* transcript in the fibroblasts of the *COX8A* patient. From *left* to *right*: molecular weight marker, brain, liver, skeletal muscle, kidney, pancreas, lung, placenta, testis, heart, fibroblasts from the *COX8A* patient, control fibroblasts, molecular weight marker. (**C**) Sequence of the *COX8A* cDNA from the index patient (mut, upper sequence) and of a control (wt, lower sequence). The loss of 49 nucleotides by aberrant splicing at a downstream cryptic AG splice acceptor site is indicated.

ubiquitous expression of *COX8A*, its transcript was detectable in all investigated tissues, while the *COX8C* transcript was only observed in pancreas, lung, placenta, and testis. A shorter *COX8A*-specific PCR product was present in fibroblasts of the *COX8A* patient (Fig. 3B, asterisk), indicating aberrant splicing. Quantitative measurements by real-time PCR (normalized to the transcript abundance of *PMPCA*, the gene for a housekeeping protein, mitochondrial processing peptidase) showed that the amount of the aberrant splice product was ~20-fold lower than the amount of the normal transcript in controls (patient, 0.089 ± 0.006; control, 1.74 ± 0.14). Despite the lack of normal *COX8A* transcript in the patient's sample, no change of the *COX8C* transcripts was noted (patient, $3.5 \times 10^{-4} \pm 0.2 \times 10^{-4}$; control, $4.9 \times 10^{-4} \pm 0.4 \times 10^{-4}$; values normalized to *PMPCA*).

To determine the exact nature of the aberrant splicing, we sequenced the transcript from the patient and compared it to a *COX8A* transcript sequence from a control (Fig. 3C). As the c.115-1G>C splice site mutation disrupted the regular AG splice acceptor site at the end of intron 1, aberrant splicing occurred at a cryptic AG splice acceptor site in exon 2, which led to the removal of 49 nucleotides. This deletion results in a shift of the reading frame for the entire exon 2 (Fig. 3C). As exon 2 encodes the 31 C-terminal amino acids of the 44 amino acid-long mature peptide, the translated mutant protein is very likely not functional. This and the low abundance of the mutated transcript explain the severe functional effect leading to only ~10% wild-type COX activity in skeletal muscle and fibroblasts.

For several small structural subunits of COX, it has been reported that their loss resulted in decreased amounts of the entire complex (Massa *et al.*, 2008; Indrieri *et al.*, 2012; Abdulhag *et al.*, 2015). As COX8A is the smallest structural subunit of COX, we were interested to see whether this was also the case for COX8A. To this end, we determined the steady-state amounts of the fully assembled COX complex in skeletal muscle mitochondrial fractions by blue native polyacrylamide gel electrophoresis (PAGE) (Fig. 4A). A marked reduction of the COX complex in the absence of any detectable subcomplexes was observed with antibodies against MT-CO1, COX4 and COX5A at comparable immunoreactivity against SDHA. As the small nuclear subunits are added to the complex at the last stage of its assembly (Mick *et al.*, 2011), this indicates that a severely impaired stability of the fully assembled COX complex in the absence of functional COX8A protein is the molecular cause for the reduced enzymatic activity in the index patient.

To verify the causative role of the loss of COX8A in the observed isolated COX deficiency, we used a lentiviral system in the patient's fibroblasts to express the wild-type COX8A protein C-terminally tagged with myc-DDK. At maximal virus load, a ~60% transduction efficiency was observed, as estimated by DDK immunoreactivity. Opposite to the sample transfected with the empty virus (Fig. 4D), in the COX8A-transduced sample, a high proportion of fibroblasts showed a typical mitochondrial pattern of MT-CO1 immunoreactivity (Fig. 4G), and this co-localized with the NDUFS5 (complex I) signal (Fig. 4H). The proportion of MT-CO1 immunoreactive fibroblasts strongly correlated with that of DDK-positive fibroblasts in different experiments with varying virus amounts (Fig. 4B). In functional activity assays on fibroblast homogenates, viral expression of COX8A caused a substantial increase of COX activity reaching almost 67% of the control activity and correlated with the percentage of transduced cells and the percentage of MT-CO1 immunoreactive cells (Fig. 4B).

Discussion

The nuclear-encoded subunits of COX complex are small and surround the catalytic core of the enzyme that comprises three mitochondrial-encoded subunits (Capaldi, 1990). Their number varies in different organisms. As the bacterial enzyme with only the three catalytic subunits is fully functional, the precise roles of the nuclear subunits in the eukaryotic enzyme are not well understood. However, it is believed that they are involved in the regulation and assembly of the complex (Mick *et al.*, 2011). Accordingly, isolated COX deficiency underlying human disease has been reported to be associated with pathogenic mutations in some of these nuclear genes. The spectrum of phenotypes described in deficiencies of structural subunits of COX is heterogeneous. A *COX6A1* mutation was found to cause axonal or mixed form of Charcot–Marie–Tooth disease (Tamiya *et al.*, 2014), mutated *COX4I2* leads to exocrine pancreatic insufficiency and dyserythropoetic anaemia (Shteyer *et al.*, 2009), and COX7B deficiency manifests in microphthalmia with linear skin lesions (Indrieri *et al.*, 2012). The phenotype of the COX8A patient reported here, a Leigh-like syndrome associated with leukodystrophy and severe epilepsy, most closely resembles the severe encephalopathy described for mutations of the *NDUFA4* (Pitceathly *et al.*, 2013) and *COX6B1* (Massa *et al.*, 2008; Abdulhag *et al.*, 2015) genes, although the residual activities of COX in skeletal muscle and fibroblasts in our patient were considerably lower.

The COX8A protein is the smallest subunit of the COX complex—the mature human protein contains only 44 amino acids. Very little is known about its precise function. It has been presumably added to the entire COX complex before the radiation of animals (Pierron *et al.*, 2012). Mammals are known to express three COX VIII isoforms (COX8A, COX8B and COX8C) (Hüttemann *et al.*, 2003) although COX8B has been silenced in catarrhines, including primates (Goldberg *et al.*, 2003). Interestingly, on loss of COX8A we did not observe any adaptive change in expression of the still remaining isoform COX8C or even an adaptive proliferation of mitochondria, which is frequently seen in mitochondrial DNA disorders (Sebastiani *et al.*, 2007).

The following functional data are consistent with this mutation to be the cause of the isolated COX deficiency and highlight the role of the COX8A subunit for the stability of COX. First, on the transcript level we detected in patient fibroblasts a shorter *COX8A* mRNA. The shorter mRNA molecule is the result of a deletion of 49 nucleotides from exon 2, due to aberrant splicing at a downstream cryptic AG splice acceptor site. This results in a shift of the reading frame for the retained remainder of exon 2 (p.Glu39Argfs*27). Presumably due to the lower efficiency of splicing at the new AG splice acceptor site [the maximum entropy score (Yeo *et al.*, 2004) is 7.87 at the new site as opposed to 10.03 at the wild-type site] the amount of mutated *COX8A* transcripts was ~20-fold reduced in comparison to wild-type transcripts in controls. Second, on the protein level the mutation led to a dramatic decrease of stability of the fully assembled COX complex, as detected in blue native PAGE of mitochondrial fractions

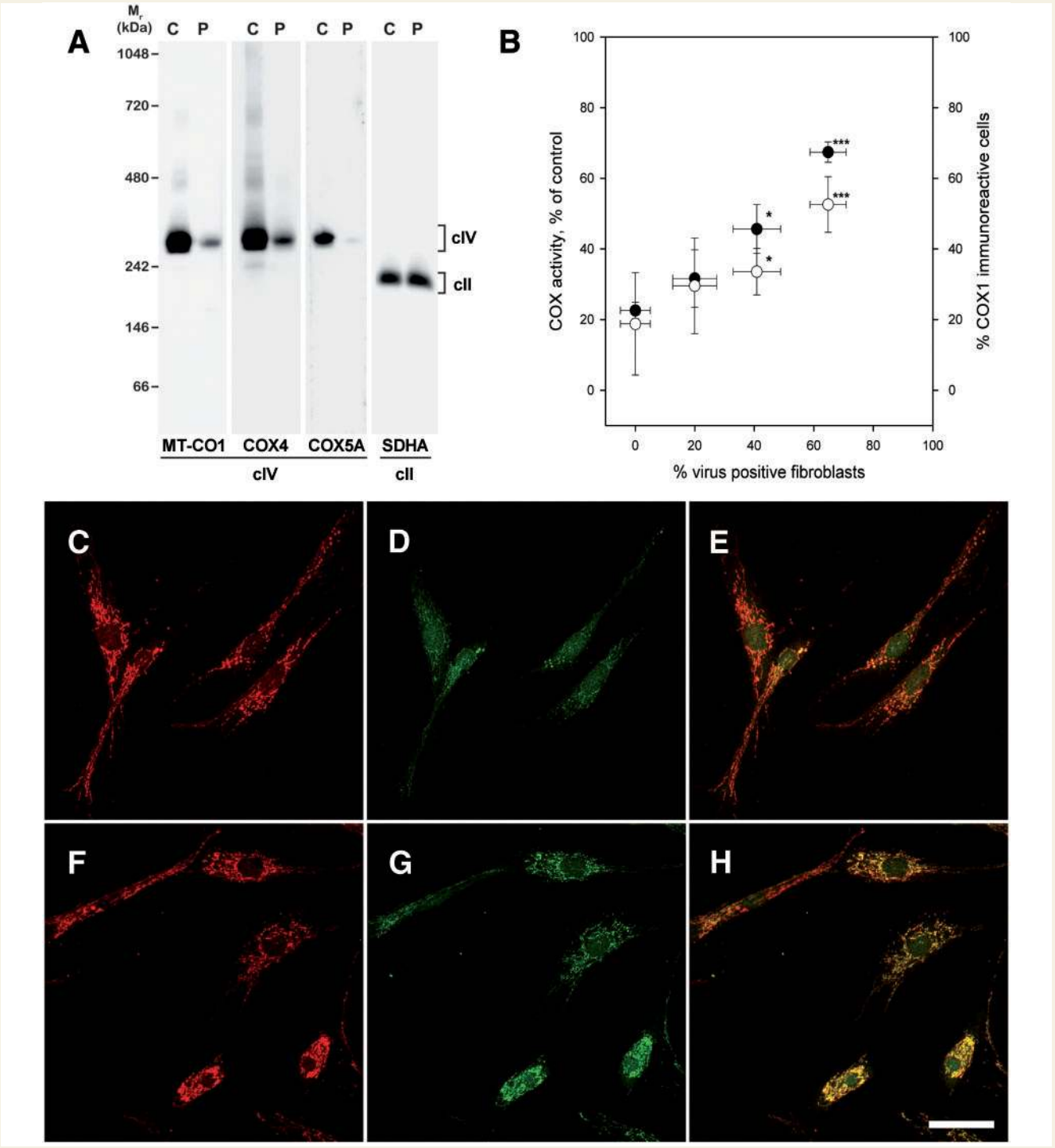

Figure 4 Blue native PAGE of mitochondrial fractions from patient's skeletal muscle (A) and lentiviral rescue of COX immunoreactivity (C–H) and activity (B) in the patient's fibroblasts. (**A**) Western blots of blue native PAGEs from mitochondrial fractions of a control muscle biopsy (C) and the patient's muscle biopsy (P) developed with antibodies against MT-CO1, COX4, COX5A and SDHA. The quantification of ratios of band intensities for MT-CO1 and SDHA from SDS PAGEs revealed in the patient's muscle 15.9 ± 1.2% of intensities of control muscle ($n = 3$). (**B**) Rescue of COX activity by lentiviral expression of wild-type COX8A in the patient's fibroblasts. Filled circles = COX activity (in per cent of activity in control fibroblasts) plotted versus percentage of transduced cells as estimated by DDK immunoreactivity. Open circles = MT-CO1 immunoreactivity plotted versus percentage of transduced cells as estimated by DDK immunoreactivity. The transduction of control fibroblasts with the COX8A-containing virus had no significant effect on COX activity, as the activity of control cells was 98 ± 17 mU/mg protein, and that of COX8A containing virus transduced cells 119 ± 31 mU/mg protein (average of two independent transductions of two control fibroblast lines). *$P < 0.05$ versus cell transduced with a control virus; ***$P < 0.001$ versus cell transduced with a control virus (*t*-test). (**C–E**) Index patient's fibroblasts transduced with a control virus. (**F–H**) Index patient's fibroblasts transduced with a wild-type COX8A containing virus. (**C** and **F**) NDUFS5 (complex I) immunoreactivity (red); (**D** and **G**) MT-CO1 (COX) immunoreactivity (green); (**E** and **H**) overlay of *left* and *middle* panels. Scale bar = 50 μm.

from skeletal muscle and by largely reduced immunoreactivity of fibroblasts with antibodies against COX subunit 1. Third, by lentiviral transduction of patient fibroblasts with wild-type *COX8A* we were able to rescue both COX complex stability and activity.

Summarizing, with our data we were able to show that the ubiquitously expressed small COX8A protein, which is present in the animal COX complex only, is not an activity regulating accessory protein, but is essential for the stability of the entire human COX complex.

Acknowledgements

The excellent technical assistance of Karin Kappes-Horn and Susanne Beyer is gratefully acknowledged.

Funding

This work was supported by the Deutsche Forschungsgemeinschaft (KU 911/21-1 to W.S.K., and ZS 99/3-1 to G.Z.), and the European Community (FP7 project EpiPGX, grant 279062 to W.S.K.). H.N. is member of the excellence cluster ImmunoSensation funded by the Deutsche Forschungsgemeinschaft.

Supplementary material

Supplementary material is available at *Brain* online.

References

Abdulhag UN, Soiferman D, Schueler-Furman O, Miller C, Shaag A, Elpeleg O, et al. Mitochondrial complex IV deficiency, caused by mutated COX6B1, is associated with encephalomyopathy, hydrocephalus and cardiomyopathy. Eur J Hum Genet 2015; 23: 159–64.

Brakebusch C, Seidenbecher CI, Asztely F, Rauch U, Matthies H, Meyer H, et al. Brevican-deficient mice display impaired hippocampal CA1 long-term potentiation but show no obvious deficits in learning and memory. Mol Cell Biol 2002; 22: 7417–27.

Capaldi RA. Structure and function of cytochrome c oxidase. Annu Rev Biochem 1990; 59: 569–96.

Dubowitz V, Sewry CA, editors. Muscle biopsy: a practical approach, 3rd edn. Philadelphia: Saunders Elsevier; 2007.

Goldberg A, Wildman DE, Schmidt TR, Hüttemann M, Goodman M, Weiss ML, et al. Adaptive evolution of cytochrome c oxidase subunit VIII in anthropoid primates. Proc Natl Acad Sci USA 2003; 100: 5873–8.

Hüttemann M, Schmidt TR, Grossman LI. A third isoform of cytochrome c oxidase subunit VIII is present in mammals. Gene 2003; 312: 95–102.

Indrieri A, van Rahden VA, Tiranti V, Morleo M, Iaconis D, Tammaro R, et al. Mutations in COX7B cause microphthalmia with linear skin lesions, an unconventional mitochondrial disease. Am J Hum Genet 2012; 91: 942–9.

Kuznetsov AV, Winkler K, Kirches E, Lins H, Feistner H, Kunz WS. Application of inhibitor titrations for the detection of oxidative phosphorylation defects in saponin-skinned muscle fibers of patients with mitochondrial diseases. Biochim Biophys Acta 1997; 1360: 142–50.

Massa V, Fernandez-Vizarra E, Alshahwan S, Bakhsh E, Goffrini P, Ferrero I, et al. Severe infantile encephalomyopathy caused by a mutation in COX6B1, a nucleus-encoded subunit of cytochrome c oxidase. Am J Hum Genet 2008; 82: 1281–9.

Mick DU, Fox TD, Rehling P. Inventory control: cytochrome c oxidase assembly regulates mitochondrial translation. Nat Rev Mol Cell Biol 2011; 12: 14–20.

Miller SA, Dykes DD, Polesky HF. A simple salting out procedure for extracting DNA from human nucleated cells. Nucleic Acids Res 1988; 16: 1215.

Pierron D, Wildman DE, Hüttemann M, Markondapatnaikuni GC, Aras S, Grossman LI. Cytochrome c oxidase: evolution of control via nuclear subunit addition. Biochim Biophys Acta 2012; 1817: 590–7.

Pitceathly RD, Rahman S, Wedatilake Y, Polke JM, Cirak S, Foley AR, et al. NDUFA4 mutations underlie dysfunction of a cytochrome c oxidase subunit linked to human neurological disease. Cell Rep 2013; 3: 1795–805.

Sebastiani M, Giordano C, Nediani C, Travaglini C, Borchi E, Zani M, et al. Induction of mitochondrial biogenesis is a maladaptive mechanism in mitochondrial cardiomyopathies. J Am Coll Cardiol 2007; 50: 1362–9.

Shteyer E, Saada A, Shaag A, Al-Hijawi FA, Kidess R, Revel-Vilk S, et al. Exocrine pancreatic insufficiency, dyserythropoeitic anemia, and calvarial hyperostosis are caused by a mutation in the COX4I2 gene. Am J Hum Genet 2009; 84: 412–7.

Soto IC, Fontanesi F, Liu J, Barrientos A. Biogenesis and assembly of eukaryotic cytochrome c oxidase catalytic core. Biochim Biophys Acta 2012; 1817: 883–97.

Tamiya G, Makino S, Hayashi M, Abe A, Numakura C, Ueki M, et al. A mutation of COX6A1 causes a recessive axonal or mixed form of Charcot-Marie-Tooth disease. Am J Hum Genet 2014; 95: 294–300.

Wiedemann FR, Vielhaber S, Schröder R, Elger CE, Kunz WS. Evaluation of methods for the determination of mitochondrial respiratory chain enzyme activities in human skeletal muscle samples. Anal Biochem 2000; 279: 55–60.

Yeo G, Burge CB. Maximum entropy modeling of short sequence motifs with applications to RNA splicing signals. J Comput Biol 2004; 11: 377–94.